Hilger, K. & C. J. Fiebach. (2019). Supporting information for "ADHD Symptoms are Associated with the Modular Structure of IntrinsicvBrain Networks in a Representative Sample of Healthy Adults. *Network Neuroscience*. Advance publication. https://doi.org/10.1162/netn_a_00083

ADHD-Symptoms in Healthy Adults are Associated with the Modular Structure of Intrinsic Brain Networks

Kirsten Hilger[1,2*], Christian J. Fiebach[1,2,3]

[1] Department of Psychology, Goethe University Frankfurt, Frankfurt am Main, Germany
[2] IDeA Center for Individual Development and Adaptive Education, Frankfurt am Main, Germany
[3] Brain Imaging Center, Goethe University Frankfurt, Frankfurt am Main, Germany

Network Neuroscience

SUPPLEMENTARY MATERIAL

* Corresponding author:

Dr. Kirsten Hilger
Goethe University
Department of Psychology
Theodor-W.-Adorno-Platz 6, PEG
D-60323 Frankfurt am Main
Phone: +49 (0)69 / 798 - 35345
hilger@psych.uni-frankfurt.de

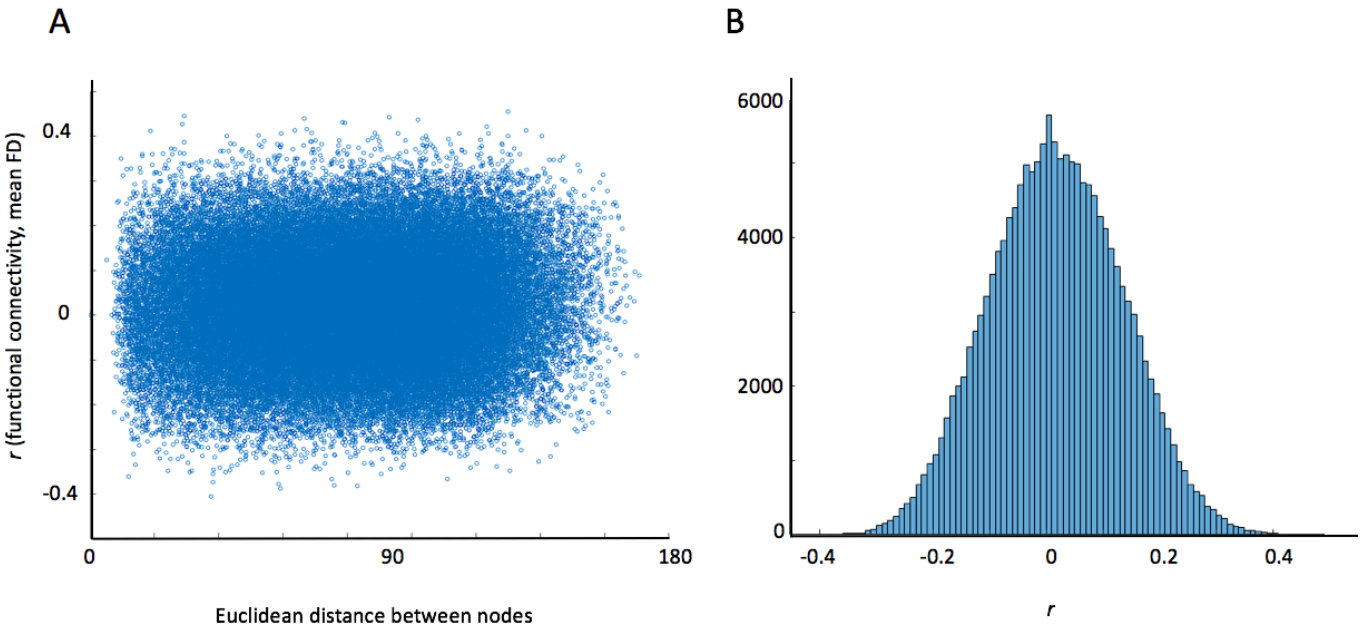

Supplementary Figure S1. Check for distance-dependent influences of in-scanner head motion on functional connectivity values. A, Scatterplot illustrating the correlation between each edge's functional connectivity strength and mean framewise displacement (*y*-axis) in dependency of Euclidean distance between the respective nodes of this edge (in mm, *x*-axis). B, Histogram of the correlation scores for the association between mean framewise displacement and functional connectivity values. FD, mean framewise displacement; *r*, Pearson correlation. Functional connectivity values are based on the 400-node parcellation of Schaefer et al. (2018).

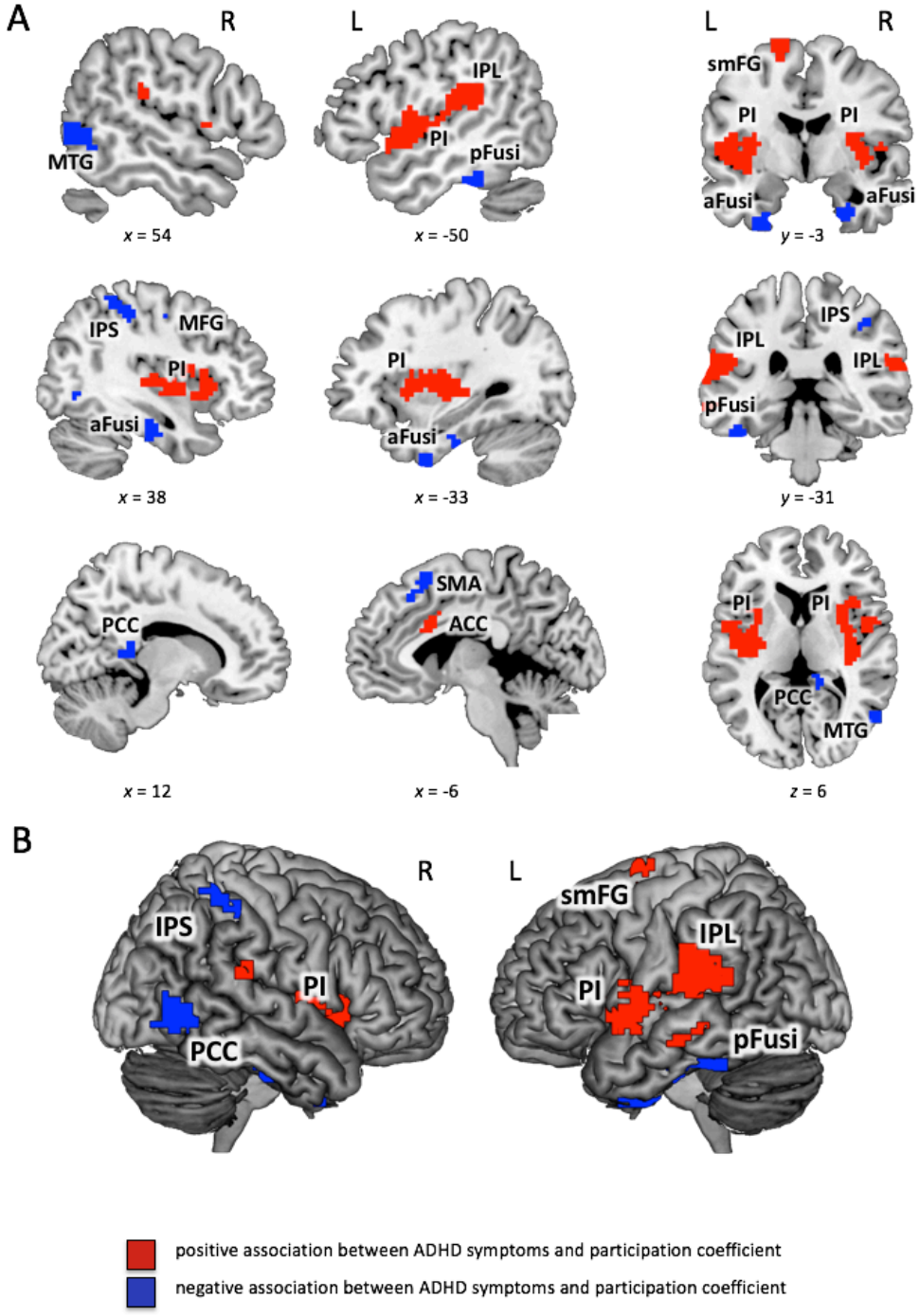

Supplementary Figure S2. Significant associations between Conners' ADHD Index and participation coefficient controlled for number of low-motion frames (rather than mean framewise displacement; see Post-Hoc Analyses in the Results Section of the Main Text, and Supplementary Table S6). *Participation coefficient* p_i (see Methods for details) was calculated for binarized and proportionally thresholded graphs using five thresholds (graphs were defined by the top 10%, 15%, 20%, 25%, or 30% of strongest edges). Input for analyses were the individual mean maps for *participation coefficient* p_i, which were calculated by averaging across these five thresholds for each participant separately. Statistic parametric maps of *participation coefficient* p_i are shown at a voxel-level threshold of $p < .005$ (uncorrected) combined with a cluster-level threshold of $k > 26$ voxels, corresponding to an overall family-wise error corrected threshold of $p < .05$ (see Methods). **(A)** Slice view; the *x*-, *y*-, and *z*-coordinates represent coordinates of the Montreal Neurological Institute template brain (MNI152).

(B) Render view; projection to the surface of the brain, search depth 12 voxels. PI, posterior insula; IPL, inferior parietal lobe; IPS, intraparietal sulcus; ACC, anterior cingulate cortex; MFG, middle frontal gyrus; SMA, supplementary motor area; aFusi, anterior fusiform gyrus; pFusi, posterior fusiform gyrus; PCC, posterior cingulate cortex; MTG, middle temporal gyrus; smFG, superior medial frontal gyrus.

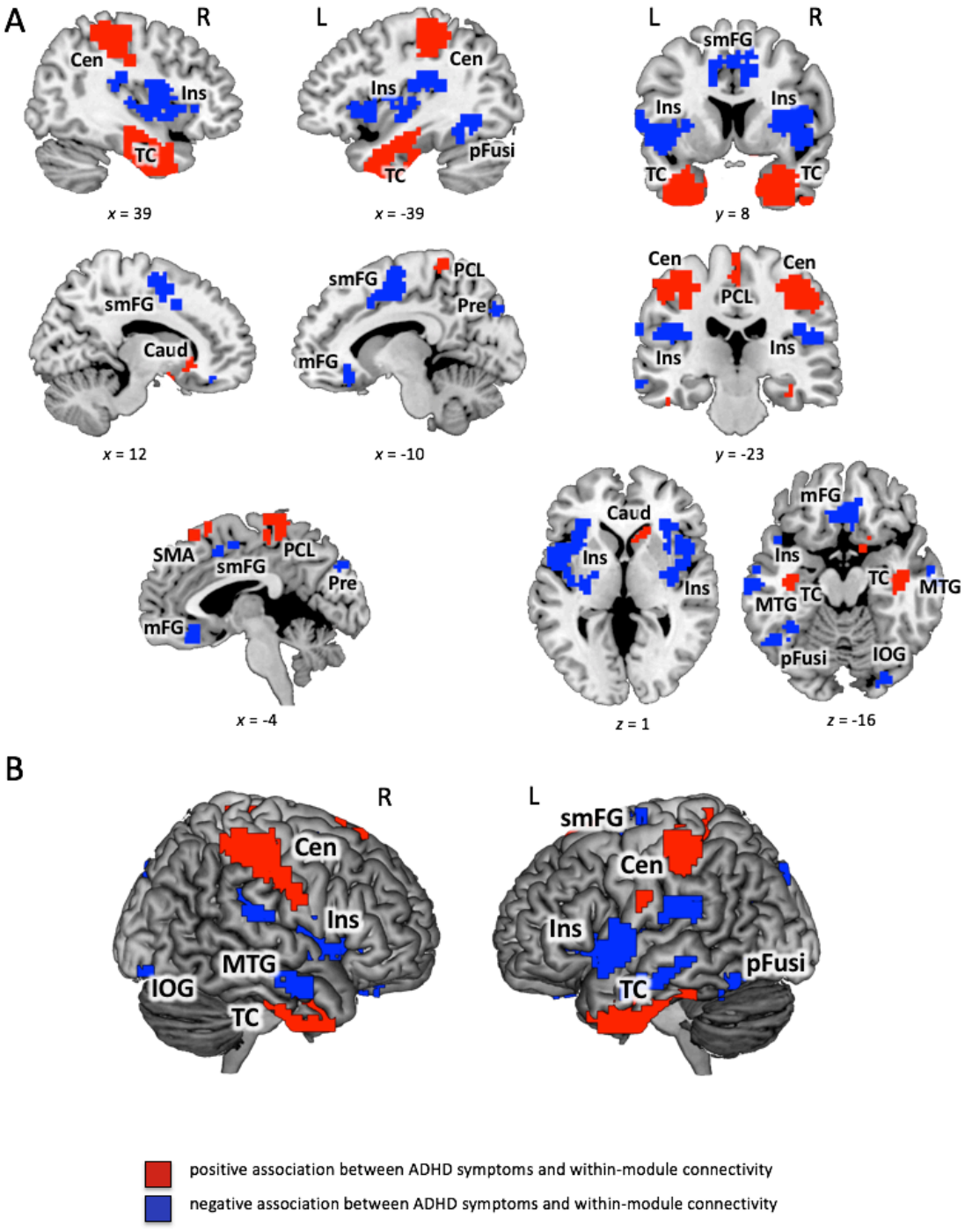

Supplementary Figure S3. Significant associations between Conners' ADHD Index and within-module degree controlled for number of low-motion frames (rather than mean framewise displacement; see Post-Hoc Analyses in the Results Section of the Main Text, and Supplementary Table S7). *Within-module degree* z_i (see Methods for details) was calculated for binarized and proportionally thresholded graphs using five thresholds (graphs were defined by the top 10%, 15%, 20%, 25%, or 30% of strongest edges). Input for analyses was the individual mean maps for *within-module degree* z_i, which were calculated by averaging across these five thresholds for each participant separately. Statistic parametric maps of *within-module degree* z_i are shown at a voxel-level threshold of $p < .005$ (uncorrected) combined with a cluster-level threshold of $k > 26$ voxels, corresponding to an overall family-wise error corrected threshold of $p < .05$ (see Methods). **(A)** Slice view; the *x*-, *y*-, and *z*-coordinates represent coordinates of the Montreal Neurological Institute template brain (MNI152). **(B)** Render view; projection to the surface of the brain, search depth 12 voxel. TC, temporal cluster comprising also amygdala,

hippocampus, and parts of fusiform gyrus; Cen, central cluster spreading across central and postcentral sulci from precentral gyri and postcentral gyri to the inferior parietal lobes (comprising supramarginal gyri and anterior parts of intraparietal sulci); PCL, paracentral lobule; mFG, medial frontal gyrus; Ins, insular cluster comprising also parts of putamen, superior temporal gyrus, inferior frontal gyrus and inferior parietal lobe; MTG, middle temporal gyrus; pFusi, posterior fusiform gyrus; Pre, precuneus; IOG, inferior occipital gyrus; smFG, superior medial frontal gyrus; SMA, supplementary motor area; Caud, caudate nucleus.

Supplementary Table S1. Correlations between CAARS subscales and whole-brain characteristics of modular network organization

	$r_{part.}$	$p_{part.}$
Inattention/Memory Problems		
global modularity	.051	.387
number of modules	-.050	.400
average module size	.043	.471
variability in module size	-.033	.579
Hyperactivity/Restlessness		
global modularity	.031	.596
number of modules	.007	.912
average module size	-.024	.681
variability in module size	-.010	.863
Impulsivity/Emotional Lability		
global modularity	.082	.166
number of modules	.037	.537
average module size	-.055	.356
variability in module size	-.019	.747
Self-Concept Problems		
global modularity	.147	.013
number of modules	-.062	.300
average module size	.061	.307
variability in module size	.118	.046

$r_{part.}$, Pearson's correlation coefficient for the partial correlation controlling for effects of age, sex, handedness, mean framewise displacement, and Full Scale Intelligence Quotient; $p_{part.}$, p-value of significance for the partial-correlation.

Supplementary Table S2. Correlations between CAARS subscales and proportions of node type within the whole brain

	$r_{part.}$	$p_{part.}$
Inattention/Memory Problems		
ultra-peripheral nodes	.053	.375
peripheral nodes	.024	.686
non-hub connector nodes	-.019	.751
non-hub kinless nodes	-.07	.239
provincial hubs	.025	.675
connector hubs	.009	.886
kinless hubs	-.096	.107
Hyperactivity/Restlessness		
ultra-peripheral nodes	.061	.307
peripheral nodes	-.026	.658
non-hub connector nodes	.010	.871
non-hub kinless nodes	-.006	.916
provincial hubs	-.042	.480
connector hubs	.048	.418
kinless hubs	-.074	.213
Impulsivity/Emotional Lability		
ultra-peripheral nodes	.115	.052
peripheral nodes	-.038	.518
non-hub connector nodes	.025	.675
non-hub kinless nodes	-.038	.52
provincial hubs	-.015	.800
connector hubs	.003	.956
kinless hubs	-.063	.285
Self-Concept Problems		
ultra-peripheral nodes	.042	.480
peripheral nodes	.068	.251
non-hub connector nodes	-.127	.032
non-hub kinless nodes	-.080	.180
provincial hubs	.015	.802
connector hubs	-.026	.656
kinless hubs	.034	.570

$r_{part.}$, Pearson's correlation coefficient for the partial correlation controlling for effects of age, sex, handedness, mean framewise displacement, and Full Scale Intelligence Quotient; $p_{part.}$, p-value of significance for the partial-correlation.

Supplementary Table S3. Correlations between Conner's ADHD Index and functional connectivity strength within/between canonical brain networks

	VIS	SOM	DAN	VAN	LIM	FPN	DMN
VIS	.011						
	(.847)	-	-	-	-	-	-
SOM	.012	.007					
	(.833)	(.901)	-	-	-	-	-
DAN	.016	.016	.021				
	(.782)	(.784)	(.717)	-	-	-	-
VAN	.035	.024	.107	.031			
	(.552)	(.684)	(.069)	(.591)	-	-	-
LIM	.024	.004	.043	.084	-.010		
	(.675)	(.939)	(.463)	(.635)	(.866)	-	-
FPN	-.015	-.011	.028	.050	-.022	.034	
	(.794)	(.848)	(.635)	(.395)	(-.702)	(.561)	-
DMN	-.086	-.092	-.102	-.061	-.044	-.017	.113
	(.142)	(.118)	(.084)	(.304)	(.449)	(.775)	(.056)

Pearson's correlation coefficient for the partial correlation between functional connectivity strength and ADHD symptoms controlling for effects of age, sex, handedness, mean framewise displacement, and Full Scale Intelligence Quotient; corresponding *p*-values are depicted in brackets; VIS, visual network; SOM, somato-motor network, DAN, dorsal attention network, VAN, ventral attention network, LIM, limbic network, FPN, frontoparietal network, DMN, default-mode network (Yeo et al., 2011).

Supplementary Table S4. Rank position of ADHD symptoms-related brain regions, relative to the whole-brain distribution of *participation coefficient* p_i and *within-module degree* z_i

Brain Region	BA	Hem	rank position p_i	rank position z_i
positive association with p_i				
posterior insula*	13	L	68.66	79.43
posterior insula, putamen*	13	R	70.97	79.92
anterior cingulate cortex	24	L	61.91	50.86
superior medial frontal gyrus*	6	L	43.39	42.40
inferior parietal lobe*	40	L	50.75	74.80
negative association with p_i				
anterior cingulate cortex	32, 9	L	43.18	**91.12**
middle frontal gyrus	6	R	31.69	**83.95**
supplementary motor area	8, 6	L	66.32	24.55
posterior fusiform gyrus	20, 36	L	43.03	**4.17**
intraparietal sulcus*	40	R	47.94	78.98
posterior cingulate cortex		R	64.93	**1.31**
middle temporal gyrus	37, 19	R	44.64	52.68
inferior parietal lobe	40	R	35.64	40.59
positive association with z_i				
supplementary motor area	8, 6	R/L	33.31	**12.45**
temporal cortex, amygdala, hippocampus, fusiform gyrus	38, 20, 28	R	52.29	**12.64**
temporal cortex, amygdala, hippocampus, fusiform gyrus	20, 38	L	49.09	**12.38**
precentral gyrus, postcentral gyrus, inferior parietal lobe*	3, 40	R	40.72	**83.64**
precentral gyrus, postcentral gyrus, inferior parietal lobe	3, 40	L	37.86	**82.82**
paracentral lobule	6, 4	L	38.69	23.32
negative association with z_i				
medial frontal gyrus	11, 32, 25	R	50.21	41.27

anterior cingulate cortex	24	R	60.92	57.89
insula, putamen, superior temporal gyrus, inferior frontal gyrus, inferior parietal lobule*	13, 22, 40	L	57.35	71.16
insula, putamen, superior temporal gyrus, inferior frontal gyrus, inferior parietal lobule*	13, 47, 22	R	56.58	67.01
superior medial frontal gyrus*	6, 32, 24	L	52.13	77.52
midde temporal gyrus	21, 20	R	30.66	78.60
thalamus		R	57.32	25.14
thalamus		L	36.58	27.35
posterior fusiform gyrus	37, 19	L	59.31	**17.80**
posterior fusiform gyrus		R	35.77	26.18
posterior cingulate cortex	30	L	57.75	66.01
precuneus	19, 7, 31	R/L	53.49	**81.13**
inferior occipital gyrus	18	R	39.84	36.88

BA, approximate Brodmann's area; Hem, hemisphere; L, left; R, right; regions with significant effects in both measures (participation coefficient and within-module degree) are marked with an asterisk and separately listed in Table 5; rank positions < 20% or > 80% are depicted in bold letters.

Supplementary Table S5. ADHD symptoms and global modularity measures controlled for number of low-motion frames (rather than mean framewise displacement; see Post-Hoc Analyses in the Results Section of the Main Text)

	$r_{part.}$	$p_{part.}$	BF_{01}-Reg.
Whole-brain modularity measures			
global modularity	.11	.059	0.63
number of modules	-.09	.148	1.35
average module size	.08	.204	1.89
variability in module size	-.03	.626	3.13
Whole-brain proportions of node types			
ultra-peripheral nodes	.01	.824	3.80
peripheral nodes	.06	.359	2.27
non-hub connector nodes	-.07	.220	2.28
non-hub kinless nodes	-.10	.107	1.02
provincial hubs	.09	.149	1.33
connector hubs	-.07	.253	2.57
kinless hubs	-.07	.263	2.61

$r_{part.}$, Pearson's correlation coefficient for the partial correlation controlling for effects of age, sex, handedness, number of low-motion frames (FD < 0.2mm), and FSIQ; $p_{part.}$, p-value of significance for the partial-correlation; BF_{01}-Reg., Bayes Factor in favor of the null hypothesis (i.e., absence of correlation). Bayes Factors were calculated for linear regression models predicting ADHD Index values by the respective whole-brain measure of modular network organization or whole-brain proportions of node types, respectively, while effects of age, sex, handedness, number of low-motion frames (FD < 0.2mm), and FSIQ were controlled.

Supplementary Table S6. ADHD symptoms and participation coefficient controlled for age, sex, handedness, FSIQ, and number of low-motion frames (rather than mean framewise displacement, see Post-Hoc Analyses in the Results Section of the Main Text)

Brain Region	BA	Hem	x	y	z	t_{max}	*k*
positive association							
posterior insula, inferior parietal lobe	13, 40	L	-57	-36	21	5.45	840
posterior inula, putamen	13	R	36	-9	3	3.64	384
anterior cingulate cortex	24	L	-6	18	24	3.60	110
superior medial frontal gyrus	6	L	-18	-3	69	3.32	47
inferior parietal lobe	40	R	63	-30	21	3.18	33
negative association							
middle frontal gyrus	6	R	33	-12	45	2.97	31
supplementary motor area	8, 6	L	-6	18	57	3.87	40
anterior fusiform gyrus	28, 38	R	27	6	-39	3.34	79
anterior fusiform gyrus	20, 36	L	-30	3	-39	3.25	63
posterior fusiform gyrus	20, 37	L	-48	-33	-27	4.09	77
posterior fusiform gyrus	20	R	42	-18	-27	3.70	46
intraparietal sulcus	40	R	33	-36	48	3.38	91
posterior cingulate cortex		R	12	-39	9	3.84	27
middle temporal gyrus	37, 19	R	57	-63	0	3.71	105

BA, approximate Brodmann's area; Hem, hemisphere; L, left; R, right; coordinates refer to the Montreal Neurological Institute template brain (MNI); t_{max}, maximum *t* statistic in the cluster; *k*, cluster size in voxels of size 3 x 3 x 3 mm.

Supplementary Table S7. ADHD symptoms and within-module degree controlled for age, sex, handedness, FSIQ, and number of low-motion frames (rather than mean framewise displacement, see Post-Hoc Analyses in the Results Section of the Main Text)

Brain Region	BA	Hem	x	y	z	t_{max}	*k*
positive association							
supplementary motor area	8, 6	R/L	0	30	60	3.20	42
caudate		R	15	24	-6	3.90	39
temporal cortex, amygdala, hippocampus, fusiform gyrus	38, 20, 28	R	33	6	-30	5.76	794
temporal cortex, amygdala, hippocampus, fusiform gyrus	20, 38	L	-27	-15	-33	5.15	872
precentral gyrus, postcentral gyrus, inferior parietal lobe	3, 40	R	39	-33	51	6.72	588
precentral gyrus, postcentral gyrus, inferior parietal lobe	3, 40	L	-45	-33	51	5.37	373
paracentral lobule	6, 4	L/R	0	-33	72	3.88	180
negative association							
medial frontal gyrus	11, 32, 25	R	3	30	-15	4.42	164
insula, putamen, superior temporal gyrus, inferior frontal gyrus, inferior parietal lobule	13, 22, 40	L	-48	9	-3	5.64	883
insula, putamen, superior temporal gyrus, inferior frontal gyrus, inferior parietal lobule	13, 47, 22	R	39	3	15	5.46	620
superior medial frontal gyrus	6, 32, 24	L	-12	-3	63	5.04	507
midde temporal gyrus	21, 20	R	63	-6	-21	4.48	63
midde temporal gyrus	21, 20	L	-66	-30	-6	3.78	104
cuneus/precuneus	19	R	42	-24	24	3.86	168
posterior fusiform gyrus	37, 19	L	-36	-48	-12	4.26	139
posterior cingulate cortex	30	L	-24	-66	21	3.60	27
precuneus	19, 7, 31	R/L	-12	-87	36	3.84	85
inferior occipital gyrus	18	R	27	-84	-12	3.31	30

BA, approximate Brodmann's area; Hem, hemisphere; L, left; R, right. Coordinates refer to the Montreal Neurological Institute template brain (MNI); t_{max}, maximum *t* statistic in the cluster; *k*, cluster size in voxels of size 3 x 3 x 3 mm.

Supplementary References

Yeo, B. T. T., Krienen, F. M., Sepulcre, J., Sabuncu, M. R., Lashkari, D., Hollinshead, M., … Buckner, R. L. (2011). The organization of the human cerebral cortex estimated by intrinsic functional connectivity. *Journal of Neurophysiology, 106*, 1125–1165. http://doi.org/10.1152/jn.00338.2011.